

Exploring the clustering in neutron-rich Be and B isotopes by reactions of ${}^9\text{Li}$ beam on LiF target

Nikola Vukman

Laboratory for nuclear physics
Ruder Bošković Institute
Bijenička c. 54, 10 000 Zagreb



nvukman@irb.hr

01.07.2022.

Clustering in (n-rich) light nuclei

- excellent "tool" for the theory test and development [1]: from Ab Initio [2-4] to Mean Field [5]
- talk by P.Li on tuesday morning - clustering and molecular structure of n-rich Be isotopes

(neutron-rich) Be and B isotopes:

- evolution of the clustering with addition of neutrons in $^{10,12}\text{Be}$ [4,5]: $\alpha\text{-Xn-}\alpha$
- role of extra proton in ^{13}B [4]: $^9\text{Li} + ^4\text{He}$, $(\alpha\text{-2n})\text{-t-}\alpha$, $^{10}\text{Be} + ^3\text{H}$
- molecular-like and cluster structures in Be, B isotopes

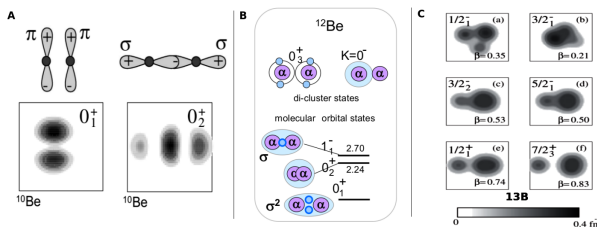


Figure 1: Schematics of molecular orbitals and two/three-center clustering in AMD formalism: **A)** ^{10}Be [2], **B)** ^{12}Be [3] and density distribution of the ^{13}B [4] ground and excited states.

- [1] M. Freer, H. Horiuchi, Y. Kanada-En'yo et al.; Rev. Mod. Phys. 90,(2018) 035004, [2] Y. Kanada-En'yo et al. Phys.Rev.C, Vol. 60, (1999) 064304, [3] Y. Kanada-En'yo et al, PTEP, Volume 2012, Issue 1 (2012) 01A202, [4] Y. Kanada-En'yo et al. PTEP, 120, 5, (2008) 917–935, [5] J. P. Ebran, E. Khan, T. Nikšić, D. Vretenar; Phys. Rev. C 90, (2014) 054329

Clustering in light nuclei: experimental approach

Cases of $^{10,12}\text{Be}$ and ^{13}B experimental study (α -clustering example): transfer [6,7], inelastic and resonant elastic scattering [8-12,15] and breakup reactions [13,14]

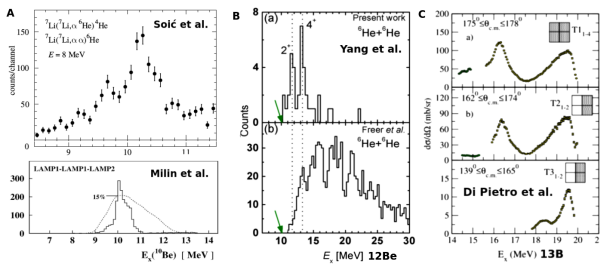


Figure 2: A) (transfer reactions ^{10}Be by Zagreb group: Soić et al. [6] and Milin et al. [7]), B) (inelastic breakup Latest results for ^{12}Be by Yang et al. [14], referencing Freer et al. [9], C) resonant elastic scattering) Latest results (published last week) for ^{13}B by Di Pietro et al. [15].

- [6] Soić et al., *Europhys. Lett.*, 34 (1), (1996) 7-12, [7] Milin et al., *Nuc. Phys. A* 753 (2005) 263–287, [8] M. Freer et al. *Phys. Rev. Lett.* 96, (2006) 042501, [9] M. Freer et al., *Phys. Rev. Lett.* 82, (1999) 1383, [10] A. Saito et al., *Nucl. Phys. A* 738, (2004) 337-341, [11] R.J. Charity et al., *Phys. Rev. C* 76, (2007) 064313, [12] M. Freer et al., *Physics Letters B* 775 (2017) 58–62, [13] M. Freer et al., *Phys. Rev. C* 63, (2001) 034301, [14] Z.H. Yang, et al., *Phys. Rev. C*, 91, (2015) 024304, [15] A. Di Pietro et al. *Phys. Let. B* 832 (2022) 137256

Experiment S1620 at TRIUMF

S1620

experiment: "Examining the helium cluster decays of the ^{12}Be excited states by triton transfer to the ^9Li beam"

spokespersons: N.Soić, M.Freer

August '17 at **TRIUMF**, Vancouver, CA.

method:

to explore the sensitivity of **transfer reactions** on the structure of the nuclei in the entrance channel

ingredients:

- ^9Li beam (75MeV) produced by ISAC-II (ISOL technique)
- LiF target (1 mg/cm^2) produced in Catania (evaporation technique)

ISAC-I and ISAC-II Facility

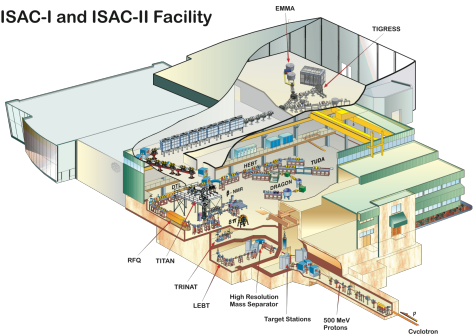


Figure 3: ISAC-II accelerator facility at TRIUMF. Targets and detector setup ("LAMP") were mounted in **TUDA** chamber.

"LAMP" detector setup

Detectors:

YY1 wedge shaped silicon strip telescopes
(16 strips in polar angle)

- $6 \times 70 \mu\text{m}$ as ΔE
- $6 \times 1500 \mu\text{m}$ as E

Geometry:

- lampshade geometry: 360° in $\Delta\phi$ and $16\text{-}48^\circ$ in $\Delta\theta$ ($2^\circ/\text{strip}$)

Particle identification:

- standard $\Delta E\text{-}E$ technique (graphical cuts)

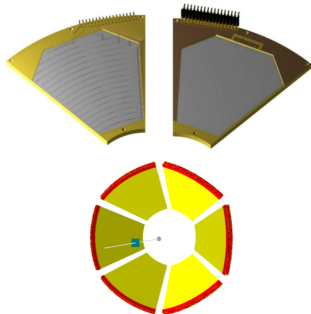


Figure 4: YY1 wedge detector [16] in LAMP telescope setup. Optimization of detection efficiency: **AUSA** MC framework [17a], while **UNISim** MC framework [17b] was used in analysis.

[16] <http://www.micronsemiconductor.co.uk/product/yy1/>, [17a] <https://git.kern.phys.au.dk/ausa/ausalib/wikis/home>,
[17b] <https://github.com/dellaquilamaster/UNISim-tool>

PID spectrum

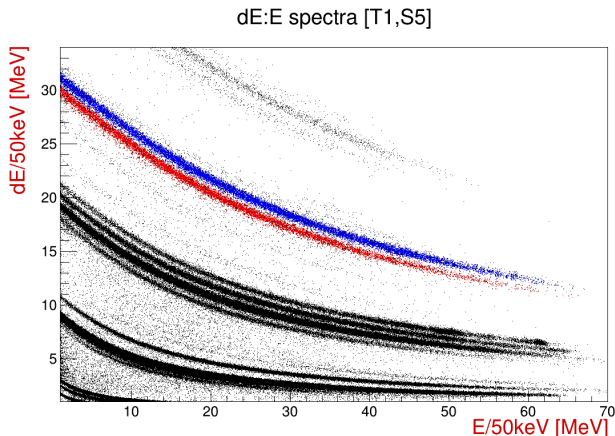
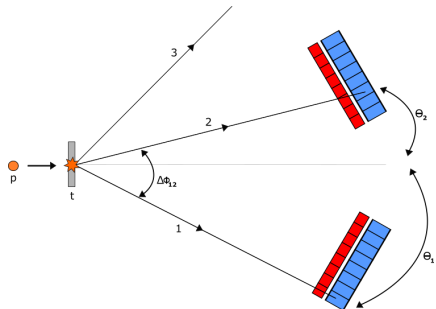


Figure 5: ΔE - E (**PID**) spectrum (zoomed) for T1-S5: example of ^{9}Be and ^{10}Be identification, the rest of the isotopes are (starting from the bottom): **H, He, Li, Be and B.**

Tree-body reactions: $t(p,12)3$



- full kinematic reconstruction:
 $p_3, E_3, Q \leftarrow \Delta\phi_{12}$ dependence
 (large uncertainty)

dT	$\Delta\phi_{12}^{nom.}$	$\Delta\phi_{12}^{real}$
0	0°	$[0^\circ, 55^\circ]$
1	60°	$[5^\circ, 115^\circ]$
2	120°	$[65^\circ, 175^\circ]$
3	180°	$[125^\circ, 180^\circ]$

Figure 6: Typical tree-body reaction:
 $t(p,12)3$, particles "1" and "2" are **detected**,
 and "3" **undetected**. Symmetrical setup:
 $\phi_1=0^\circ$, $\phi_2=\Delta\phi_{12}$.

- exit channel ID: **Catania plot +**
Q value spectra → → $\Delta\phi_{12}^{reco}$.
 $\Delta\phi_{12}^{reco} \propto f(Q, E_1, E_2, \theta_1, \theta_2,)$

$$E_{r12} \propto f(E_1, E_2, \theta_1, \theta_2, \Delta\phi_{12}) - E_{r13} \propto Q + f(E_2^{CM}) - E_{r23} \propto Q + f(E_1^{CM})$$

excitation energy: $Ex^{ij} = E_{tr.}^{ij} + E_{rel.}^{ij}$

Experimental results: ${}^7\text{Li}({}^9\text{Li}, {}^9\text{Li}{}^4\text{He}){}^3\text{H} - {}^{13}\text{B}$

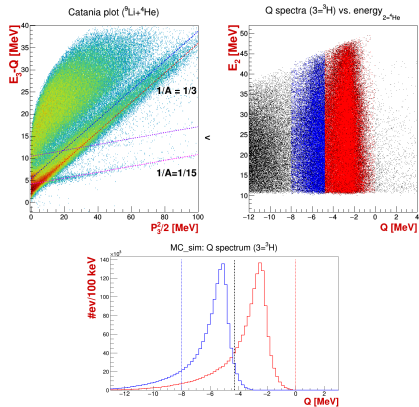
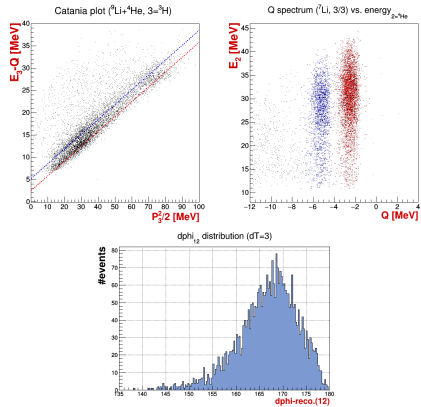


Figure 7: 3/3: a) Catania plot (slope $\sim 1/A$) and Q value spectrum for ${}^7\text{Li}({}^9\text{Li}, {}^9\text{Li}{}^4\text{He}){}^3\text{H}$ reaction.
 b) Reconstructed $\Delta\phi_{12}^{reco.}$ distribution for the $\Delta\phi_{12}^{nom.} = 180^\circ$.

Figure 8: 2/3: a) Catania plot (slope $\sim 1/A$) and Q value spectrum for ${}^7\text{Li}({}^9\text{Li}, {}^9\text{Li}{}^4\text{He}){}^3\text{H}$ reaction.
 b) Data selection QC test (UNISim MC framework).

Experimental results: $^{13}\text{B} \rightarrow {}^9\text{Li} + {}^4\text{He}$ (on ${}^7\text{Li}$)

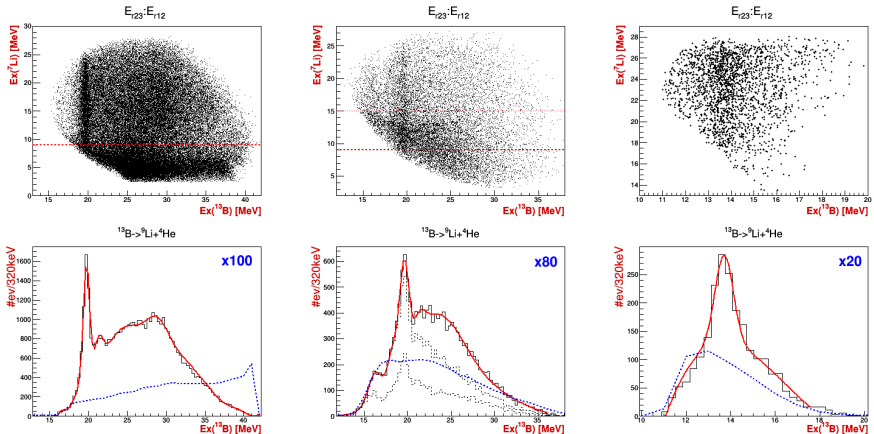


Figure 9: Excitation energy spectra for the ^{13}B decays to the ${}^9\text{Li} + {}^4\text{He}$ pairs from the coincident detection of the ${}^9\text{Li} + {}^4\text{He}$ pairs in $dT=3$ (A), $dT=2$ (B) and $dT=1$ (C) telescope combinations.

Experimental results: $^{13}\text{B} \rightarrow {}^9\text{Li} + {}^4\text{He}$ - table of states

reaction ↓ Ex [MeV] →	12	13.5	16.5	18.5	19.7	21.5
${}^7\text{Li}({}^9\text{Li}, {}^9\text{Li}{}^4\text{He})_{dT=3} {}^3\text{H}$			○	○	⊗	⊗
${}^7\text{Li}({}^9\text{Li}, {}^9\text{Li}{}^4\text{He})_{dT=2} {}^3\text{H}$			⊗	○	⊗	○
${}^7\text{Li}({}^9\text{Li}, {}^9\text{Li}{}^4\text{He})_{dT=1} {}^3\text{H}$	◊	⊗	◊			
${}^7\text{Li}({}^9\text{Li}, {}^9\text{Li}{}^4\text{He})_{dT=0} {}^3\text{H}$	○	⊗				
${}^{19}\text{F}({}^9\text{Li}, {}^9\text{Li}{}^4\text{He})_{dT=3} {}^{15}\text{N}$			○	○	⊗	⊗
${}^{19}\text{F}({}^9\text{Li}, {}^9\text{Li}{}^4\text{He})_{dT=3} {}^{15}\text{N}^*$			○	○	⊗	○
${}^{19}\text{F}({}^9\text{Li}, {}^9\text{Li}{}^4\text{He})_{dT=1} {}^{15}\text{N}$		⊗	○	○	○	
${}^{19}\text{F}({}^9\text{Li}, {}^9\text{Li}{}^4\text{He})_{dT=1} {}^{15}\text{N}^*$	◊	⊗	⊗	○	○	
${}^{19}\text{F}({}^9\text{Li}, {}^9\text{Li}{}^4\text{He})_{dT=0} {}^{15}\text{N}$	⊗	⊗				
${}^{19}\text{F}({}^9\text{Li}, {}^9\text{Li}{}^4\text{He})_{dT=0} {}^{15}\text{N}^*$	○	⊗				
references	[18*]	[19, 20]	[21]	[21]	[21]	

⊗ = good statistics and fit, ○ = peaks with low statistics and/or background interference;

◊ = peaks with low statistics which were not fitted, but have a possible presence in the relative energy spectra.

- [18] A. H. Wuosmaa et al. Phys. Rev. C 90, (2014) 061301, [19] N. R. Fletcher et al. Phys. Rev. C 68, (2003) 024316,
 [20] R. J. Charity et al., Phys. Rev. C 78, (2008) 054307, [21] A. Di Pietro et al. Phys. Lett. B 832 (2022) 137256

Experimental results: $^{13}\text{B} \rightarrow ^7\text{Li} + ^6\text{He}$, $^{10}\text{Be} + ^3\text{H}$

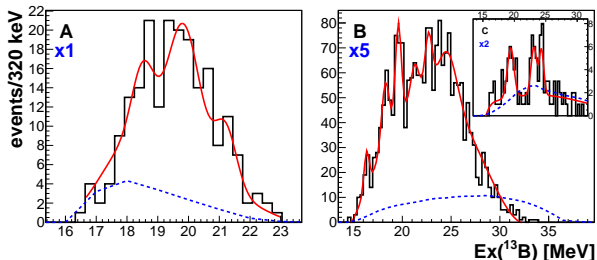


Figure 10: Excitation energy spectra for the ^{13}B decays to the: $^7\text{Li} + ^6\text{He}$ (A, dT=1) and $^{10}\text{Be} + ^3\text{H}$ (B, dT=3, C, dT=3 on ^{19}F).
note: $^7\text{Li} = \text{g.s.} + 0.48 \text{ MeV}$

reaction ↓ Ex [MeV] →	16.3	18.5	19.5	21.2	22.9	24.7
$^7\text{Li}(^9\text{Li}, ^7\text{Li} + ^6\text{He})_{dT=1} + ^3\text{H}$		⊗	⊗	○		
$^{19}\text{F}(^9\text{Li}, ^{10}\text{Be} + ^3\text{H})_{dT=3} + ^3\text{H}$	○	⊗	⊗	○	○	○
$^{19}\text{F}(^9\text{Li}, ^{10}\text{Be} + ^3\text{H})_{dT=3} + ^{15}\text{N}$	◊		⊗		⊗	⊗

⊗ = good statistics and fit, ○ = peaks with low statistics and/or background interference;

◊ = peaks with low statistics which were not fitted, but have a possible presence in the relative energy spectra.

Experimental results: $^{10}\text{Be} \rightarrow {}^4\text{He} + {}^6\text{He}$ (on ${}^7\text{Li}$)

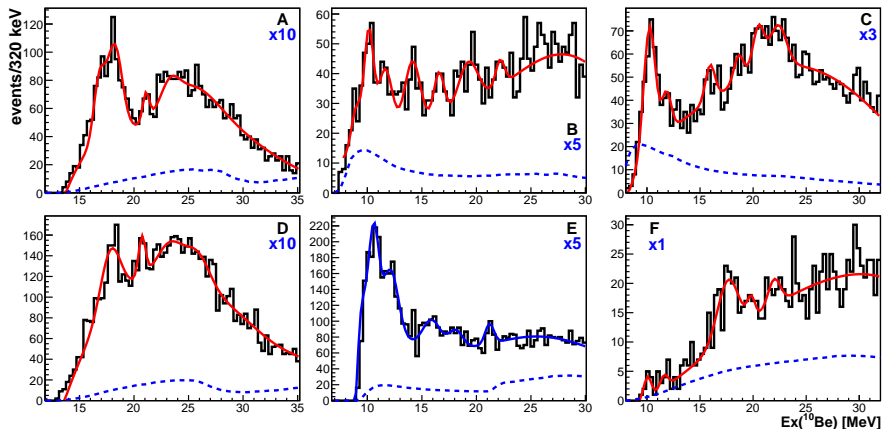


Figure 11: Excitation energy spectra for the ${}^{10}\text{Be}$ decays to the ${}^4\text{He} + {}^6\text{He}$ and ${}^4\text{He} + {}^6\text{He}^*$ (**E**) pairs from the coincident detection of the: ${}^4\text{He} + {}^6\text{He}$ (**A**-12-dT3, **B**-13-dT3, **D**-12-dT3*, **E**-13*-dT3*) and ${}^6\text{He} + {}^6\text{He}$ (**C**-13+23-dT3, **F**-13+23-dT3) pairs. Blue dashed line represents geometrical efficiency (%).

Experimental results: $^{12}\text{Be} \rightarrow {}^6\text{He} + {}^6\text{He}$ (on ${}^7\text{Li}$)

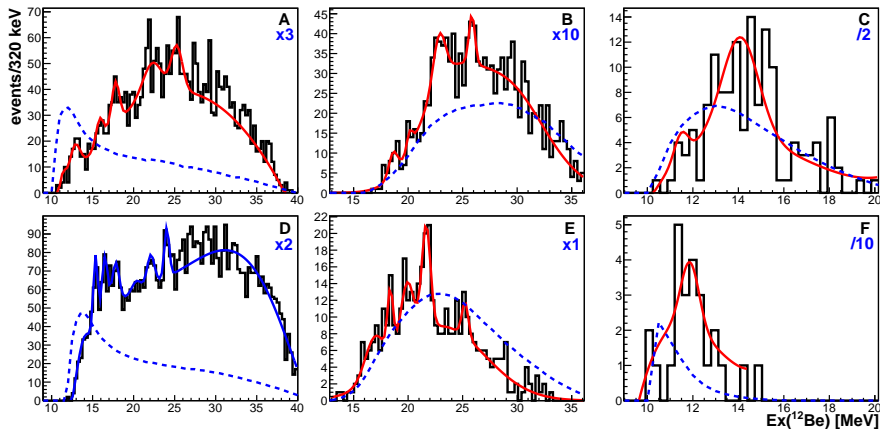


Figure 12: Excitation energy spectra for the ^{12}Be decays to the ${}^6\text{He} + {}^6\text{He}$ and ${}^6\text{He} + {}^6\text{He}^*$ (**D**) pairs from the coincident detection of the: ${}^4\text{He} + {}^6\text{He}$ (**A-23-dT3**, **D-23*-dT3***) and ${}^6\text{He} + {}^6\text{He}$ (**B-12-dT3**, **C-12-dT1**, **E-12-dT2**, **F-12-dT0**) pairs. Blue dashed line represents geometrical efficiency (%).

Experimental results: $^{12}\text{Be} \rightarrow {}^4\text{He} + {}^8\text{He}$ (on ${}^7\text{Li}$)

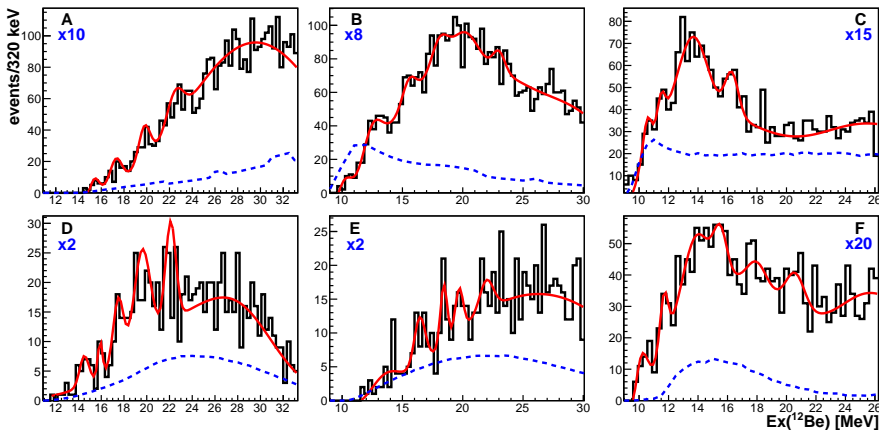


Figure 13: Excitation energy spectra for the ^{12}Be decays to the ${}^4\text{He} + {}^8\text{He}$ pairs from the coincident detection of the: ${}^4\text{He} + {}^8\text{He}$ (**A**-12-dT3, **B**-23-dT3, **D**-12-dT2, **E**-23-dT2) and ${}^4\text{He} + {}^4\text{He}$ (**C**-13+23-dT3, **H**-13+23-dT2) pairs. Blue dashed line represents geometrical efficiency (%).

Experimental results: $^{10,12}\text{Be}$ table of states

$^{10}\text{Be} \rightarrow {}^6\text{He} + {}^6\text{He}$			$^{10}\text{Be} \rightarrow {}^6\text{He} + {}^6\text{He}^*$
7.5		[1,2,5]	
9.6	✓	[2-9]	(✓)
10.2	✓	[1-6,8,10,12*]	✓
11.8	✓	[1,3-9,11]	✓
[13.5]		[5-7,11]	
(14.7)	(✓)	[11]	
16.5	✓	[11]	16.0
[17.8]/ 18.5	✓	[4*, 5*, 11]	
20.0	✓		20.8
23.0	✓		

$^{12}\text{Be} \rightarrow {}^6\text{He} + {}^6\text{He}$			$^{12}\text{Be} \rightarrow {}^6\text{He} + {}^6\text{He}^*$	$^{12}\text{Be} \rightarrow {}^4\text{He} + {}^8\text{He}$	
				[9.8]	[13,14*]
				10.3	✓ [15]
[10.9]/[11.3]		[13,14*]			[13,14*]
11.7	✓	[14,15]		12.1	✓ [15,16]
13.5	✓	[15-17]	(13.8)	13.6	✓ [15,16,17*]
(14.7)/[15.5*]	✓	[14,16,17*]	15.5	(14.5)	✓ [14,16,18]
16.1	✓	[16,17*]	16.5	15.9	✓ [14,16,18]
[17.8]/ 18.6 /[19.3]	✓	[14,16]	17.8	17.2 /[18.2]	✓ [16]
20.9	✓	[16]		19.8 /[19.2/20.7]	✓ [14,16]
(21.7)	✓	[14]			[14]
22.8	✓	[16]	22.1	22.5	✓
[24.0]/ 25.1	✓	[16]	24		

- [1] M.Milin et al., Nuc. Phys. A 753 (2005) 263-287, [2] W. Jiang et al. Phys. Rev. C 101, (2020) 031304(R), [3] N.Soto et al., Europhys. Lett., 34 (1), (1996) 7-12, [4] Hamada et al., Phys. Rev. C 49(6) (1994) 3192-3199, [5] N.Curtis et al., Phys. Rev. C 64, (2001) 044604, N.Curtis et al. Phys. Rev. C 65, (2002) 034317, N.Curtis et al. Phys. Rev. C 73, (2006) 057301 [6] D.Dell'Aquila et al. Phys. Rev. C 93, (2016) 024611, [7] N.Ashwood et al., Phys. Rev. C 68, (2003) 017603, [8] R.J.Charity et al. Phys. Rev. C 78, (2008) 054307, [9] H.G.Bohlen et al. Phys. Rev. C 75, (2007) 054604, [10] M.Freer et al. Phys. Rev. Lett. 96, (2006) 042501, [11] M.Freer et al. Phys. Rev. C 63 (2001) 034301, [12] Suzuki et al., Phys. Rev. C, 87, (2013) 054301, [13] A. Saito et al., Nucl. Phys. A 738, (2004) 337-341, [14] H.G. Bohlen et al., Phys. Atom. Nuclei (2002) 65: 603 + H.G. Bohlen et al. Nuclear Physics A738 (2004) 333-336 [15] Z.H. Yang, et al., Phys. Rev. C, 91, (2015) 024304, [16] M. Freer et al., Phys. Rev. Lett. 82, (1999) 1383, M. Freer et al., Phys. Rev. C 63, (2001) 034301, [17] R.J. Charity et al.,Phys. Rev. C 76, (2007) 064313, [18] M. Freer et al., Physics Letters B 775 (2017) 58-62

Summary

- extensive research of reactions of ^9Li beam on ^7Li and ^{19}F targets was carried out
- multinucleon (cluster) transfer reactions are suitable for populating cluster and molecular states in wide variety of nuclei (focus on $^{10,12}\text{Be}$ and ^{13}B)

^{13}B :

- support of published $^9\text{Li} + ^4\text{He}$ experimental results with 2 new states at 12 and 21.5 MeV observed
- first experimental observation of $^7\text{Li} + ^6\text{He}$ (18.5, 19.5, 21.2 MeV) and $^{10}\text{Be} + ^3\text{H}$ (16.5, 18.5, 19.5, (21.2), 22.9, 24.7 MeV) decay channels

^{10}Be :

- observation of known molecular states with new observation of states at 18.5*, 20 and 23 MeV
- data didn't indicate the existence of high-spin 13.5 MeV state
- experimental evidence of $^4\text{He} + ^6\text{He}^*$ decay ((9.6), 10.2, 11.8, 16 and 20.8 MeV states)
- support of α - $2n$ - α molecular structure

^{12}Be :

- newly observed state at 22.5 MeV in $^4\text{He} + ^8\text{He}$ channel and first exclusive measurement (decay to ^4He or ^6He) for number of states
- first experimental evidence of $^6\text{He} + ^6\text{He}^*$ decay ((13.8), 15.5, 16.5, 17.8, 22.1, (24) MeV states)
- support of α - $4n$ - α molecular structure

GENERAL:

- number of new states and/or decay channels observed in $^{10,12}\text{Be}$ and ^{13}B

Thank you DREB2022!

A special thanks to supervisor and collaborators on the experiment:

N.Soić¹, M.Freer²,

M.Alcorta³, D.Connolly³, P.Čolović¹, T.Davinson⁴, A.Di Pietro⁵,
A.Lennarz³, A.Psaltis⁶, C.Ruiz³, A.Shotter⁴, M.Uroić¹, M.Williams³

¹ Ruđer Bošković Institute, Zagreb, Croatia

² University of Birmingham, Birmingham, United Kingdom

³ TRIUMF, Vancouver, Canada

⁴ The University of Edinburgh, Edinburgh, United Kingdom

⁵ INFN Laboratori Nazionali del Sud, Catania, Italy

⁶ McMaster University, Hamilton, Canada

and colleagues from Ruđer Bošković Institute and Faculty of Science in Zagreb.

Acknowledgments: This work has been supported by the Croatian Science Foundation projects: **Sr-ETNo** (IP-2013-11-7194) and **NeRiS-Land** (HRZZ-IP-2018-01-1257), and Horizon 2020 project **PaRaDeSEC** (EK-H2020-669014).